**International Symposium on Microalloyed Steels for the Oil and Gas Industry**
*Edited by W.J. Fazackerley, P. Bordignon, K. Hulka, and F. Siciliano*
***TMS (The Minerals, Metals & Materials Society), 2007***

# DEVELOPMENT OF Q&T WELDABLE SEAMLESS PIPES OF 100 KSI GRADE

E. Anelli[1], A. Di Schino[1], G. Porcu[1], A. Izquierdo[2], H. Quintanilla[2], G. Cumino[3], M. Tivelli[4]

[1]Centro Sviluppo Materiali SpA, Rome, Italy
[2]TenarisTamsa, Veracruz, Mexico
[3]TenarisDalmine, Dalmine (BG), Italy
[4]Tenaris, Campana, Argentina

Keywords: Seamless pipes, quenching, tempering, high strength, toughness, microstructure

## Abstract

The Joint Industrial Program "Seamless 100 ksi weldable" was launched by Tenaris in June 2003 in order to address the complex design issues of high strength seamless Q&T pipes. The JIP was split into two mains phases, the first one devoted to the development and production of seamless pipes intended for deepwater top tension risers (TTR), with yield strength greater than 100 ksi (690 MPa), and the second one to evaluate their field weldability. Phase I was recently completed.

The role of chemical composition and Q&T process conditions on microstructure and precipitation was analyzed, together with relevant effects on strength and toughness, for both laboratory and industrial steels. The main microstructural features which control the strength-toughness combination of these high grade Q&T steels were identified:

- The sub-grain size is the key microstructural parameter defining the yield strength of the various materials.
- Toughness was related to the inverse square root of the packet size.
- For a given prior austenite grain size, an increase in the martensite volume fraction formed after quenching leads to a finer packet, thereby enhancing toughness.
- Fine packets and sub-grains, suitable to achieve the target strength-toughness combination, i.e YS > 690 MPa (100 ksi) and FATT < – 50 °C (– 45 °F), were obtained when the as-quenched microstructure was mainly constituted of low-C martensite (M > 60%).

These results can be exploited to establish a production route for Q&T seamless pipes for deepwater TTR in 100 ksi grade.

## Introduction

The development of deepwater oil and gas reserves is continuously facing the challenge of containing/reducing costs in all components. In this context, a key component is the riser system which has a cost quite sensitive to water depth. New technical solutions have to be explored for riser weight reduction, which will also have a significant impact on the tensioning system used to support the riser. Therefore, the availability of higher-grade weldable steel risers with a WT/OD ratio adequate to satisfy the expected collapse performance is of engineering importance.

In June 2003 Tenaris invited various oil companies to participate to a Joint Industrial Program (JIP), termed "Seamless 100 ksi Weldable", which is aimed at increasing the knowledge needed to manufacture and use quenched and tempered (Q&T) seamless pipes with minimum yield strength (YS) from 90 to 100 ksi for Top Tension Risers.

The JIP was split into two mains phases, the first one was devoted to the development and production of high strength seamless pipes intended for deepwater top tension riser (TTR), and the second one was designed to evaluate their field weldability. Phase I was recently completed.

In the light of the target properties identified by JIP partners for Q&T seamless pipes of 90 and 100 ksi grade (Table I), base concepts for a proper metallurgical design of seamless pipe were identified by metallurgical modelling, laboratory trials and industrial trials, following an approach already successfully applied for the development of X65 to X80 Q&T seamless pipes for deep water [1-3]. In particular, key aspects associated with design and manufacture of new seamless pipes for high grade risers operating at both high pressure and high axial stress are presented in this paper.

Table I. Agreed properties for Q&T seamless pipes of 90 and 100 ksi grade

| **Base material** | **90 ksi** | **100 ksi** |
|---|---|---|
| Yield strength, Rt0.5 ksi (MPa) | ≥ 90 (620) | ≥ 100 (690) |
| Yield strength, Rm ksi (MPa) | ≥ 100 (690) | ≥ 110 (760) |
| Y/T ratio | ≤0.92 | ≤0.95 |
| Elongation (%) | ≥ 20 | ≥ 18 |
| Charpy-V energy (Joules) | ≥ 100@-10 °C | ≥ 80@-10 °C |
| CTOD (mm) | ≥ 0.25@-10 °C | ≥ 0.25@-10 °C |

## Experimental

Steels and Heat Treatments

The promising chemical composition ranges and Q&T conditions were identified on the basis of Tenaris-CSM background knowledge and application of mathematical models able to predict the strength of Q&T steels [4]:

- Nb-V microalloyed steel with 1.4-1.6% Mn, and appropriate additions of Mo, Ni and Cr.
- Carbon contents from 0.07 to 0.11%, the lower the carbon content in the steel the higher the level of alloying elements that may be used.
- Carbon equivalent ranges from 0.45 to 0.58 percent.

Fine tuning was performed to identify steels and processing conditions able to develop the required combinations of strength and toughness.
Pilot hot rolling down to 16 mm and 25 mm and various Q&T treatments were carried out on two laboratory steels with chemical compositions, which mainly differ with respect to molybdenum content (Table II).

Table II. Chemical composition of laboratory heats (mass %)

| Steel | C | Mn | Si | Mo | Cr | Ni | Nb | V | Ceq | Pcm |
|---|---|---|---|---|---|---|---|---|---|---|
| S1 | 0.08 | 1.60 | 0.30 | 0.20 | 0.25 | 0.40 | 0.030 | 0.050 | 0.47 | 0.21 |
| S2 | 0.09 | 1.60 | 0.30 | 0.30 | 0.25 | 0.40 | 0.030 | 0.050 | 0.50 | 0.22 |

Austenitizing was performed in a muffle furnace at a temperature of 900 to 940 °C, followed by quenching in stirred water with a cooling rate (CR) measured by thermocouple inserted at mid-thickness of 24 to 62 °C/s, this was followed by tempering at 620 to 650°C.

Based on the laboratory results, other steels were manufactured, using as a base chemical composition 0.09%C-0.25%Si-1.5%Mn-0.025%Nb-0.05%V, with selected combinations of molybdenum, chromium and nickel contents, and minor changes for other elements (Table III). Again Q&T samples of 15-16 mm and 25 mm thickness (WT) were manufactured.

Table III. Chemical compositions of industrial steels (mass %)

| Steel | Nb | Ti | V | Ceq | Pcm |
|---|---|---|---|---|---|
| T1 | 0.029 | <0.002 | 0.06 | 0.49 | 0.22 |
| T2 | 0.026 | 0.008 | 0.04 | 0.56 | 0.23 |
| T3 | 0.025 | 0.008 | <0.005 | 0.54 | 0.24 |
| D1 | 0.026 | <0.002 | 0.07 | 0.48 | 0.22 |
| D2 | 0.026 | <0.002 | 0.06 | 0.58 | 0.26 |

Dilatometry and Quantitative Metallography

Phase transformation characteristics of the steels were determined by a dilatometer, reproducing cooling rates typical of pipe quenching.

Microstructures were observed by means of Light Microscopy (LM) and Scanning Electron Microscopy (SEM) on polished sections after 2%-nital etching. The austenite grain boundaries were revealed by etching in a saturated aqueous picric acid solution containing a few drops of a wetting agent (teepol) and HCl. The austenite grain size (AGS) was measured according to ASTM E112.

Packet and cell size were determined by the Orientation Imaging Microscopy (OIM) technique using Electron Back-Scattering Diffraction (EBSD) patterns. By means of this technique, the surface of a crystalline material with low dislocation density can be scanned and at each point the local orientation can be determined in a fully automatic way. From these measurements some microstructural characteristics of the material can be estimated, e.g. misorientations and types of grain boundaries, crystallographic orientations, etc. It is of great importance to assess the crystallographic grain size, because this parameter greatly influences the strength and the cleavage fracture resistance of ferritic steels.

Information on the nature and size of fine precipitates was obtained by transmission electron microscopy with scanning attachment and high spatial resolution energy dispersive spectrometry (TEM/STEM-EDS), using extraction replicas.

Mechanical testing

Tensile tests were performed on transverse round specimens and transverse Charpy V-notch specimens were used to determine the transition curves together with the Fracture Appearance Transition Temperature (50% FATT).

## Results and Discussion

Strength-Toughness Combination

The main results from laboratory materials in terms of strength/toughness combinations for 16 mm and 25 mm thicknesses are reported in Figures 1 and 2, respectively show that::

- The most promising Q&T materials were those manufactured with Steel S2 containing 0.29% Mo, which can achieve 100 ksi grade (YS = 680-750 MPa) in the case of 16 mm thickness with a 50%FATT of – 40 / – 50 °C.
- Additional strengthening can be achieved by increasing austenitizing temperature (*i.e.* AGS) and cooling rate.
- Toughness slightly improves with increase in tempering temperature, while the strength can be maintained to suitable levels acting on AGS and cooling rate.
- With 0.29% Mo steel S2, production of 90 ksi grade was feasible for 25 mm thick material.

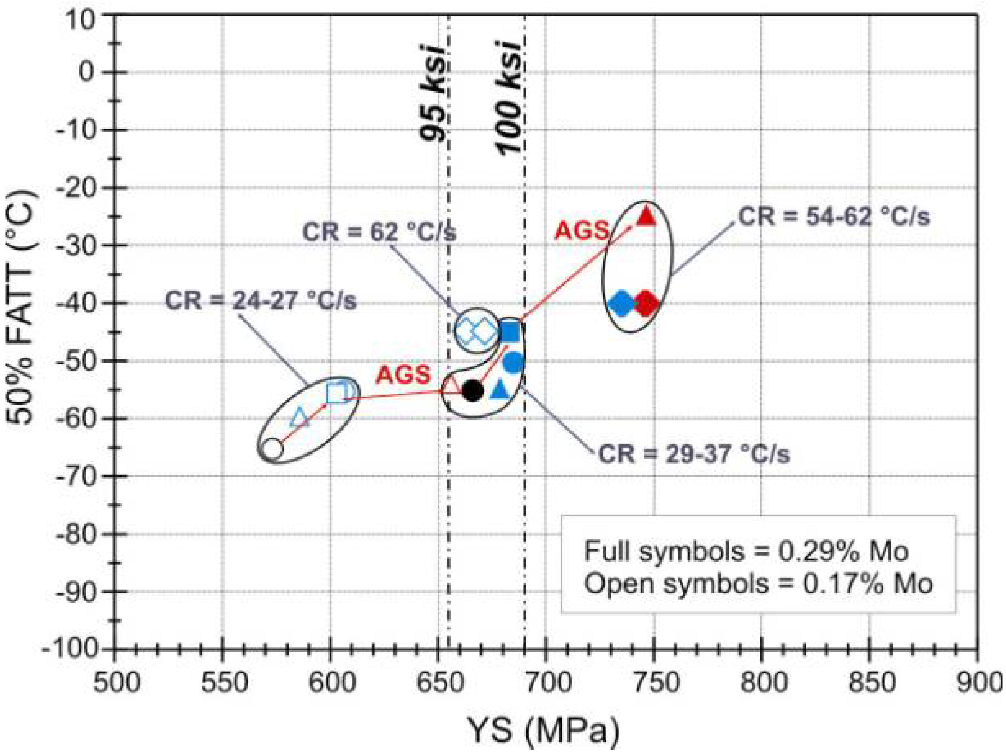


Figure 1. Strength/toughness combinations (transverse specimens) for laboratory materials (16 mm thickness). The effects of AGS and cooling rate (CR) are highlighted.

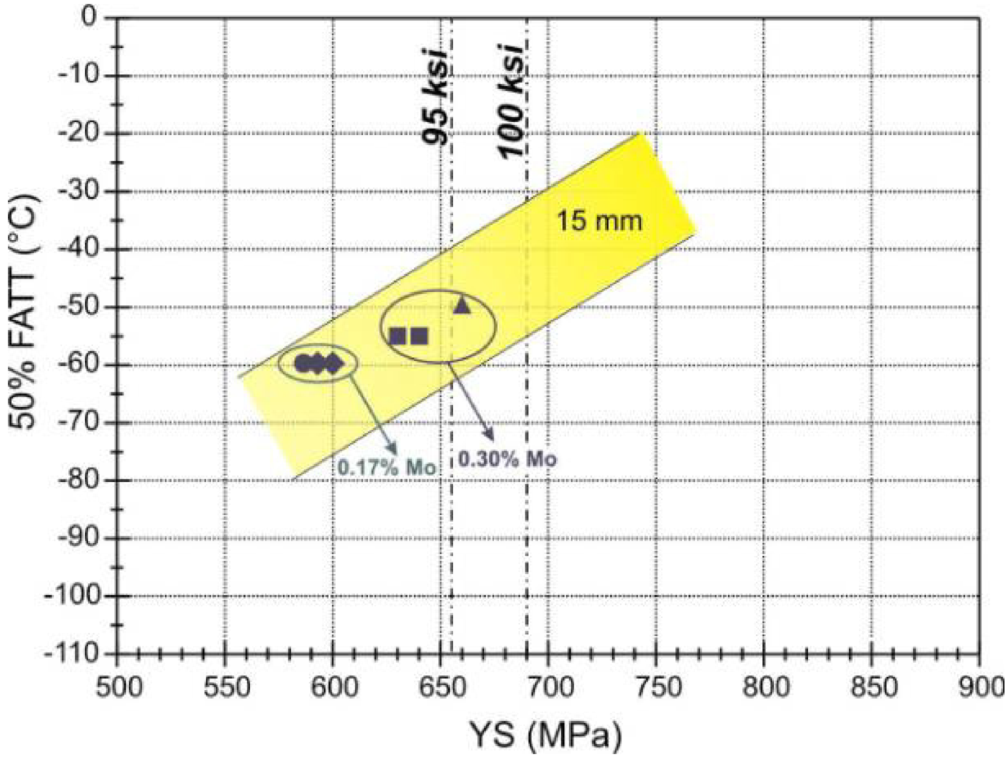


Figure 2. Strength/toughness combinations (transverse specimens) for the laboratory materials (25 mm thickness).

According to these results further steels (Table III) were included in the investigation in order to relate the strength and toughness behavior of Q&T materials to their microstructure and precipitation processes. Steels with various as-quenched microstructures, constituted of predominantly bainitic microstructure, mixed bainite-martensite and fully martensite were considered for deeper metallographic examinations.

Strength toughness combinations of the selected Q&T materials are reported in Figure 3, where also a few Q&T materials of lower grade (X65 to X80), already examined [3] are included in order to investigate a wider range of YS and 50%FATT: namely 480 MPa to 780 MPa and – 120 °C to – 5 °C, respectively.

<u>Hardenability</u>

Results from dilatometric curves are summarized in Figure 4, where martensite content is reported as a function of cooling rate for various steels with 10-12 µm AGS. For a given cooling rate during quenching, an increase of chromium and molybdenum contents allows one to achieve higher volume fractions of martensite and lowers start and finish transformation temperatures (Figure 5).

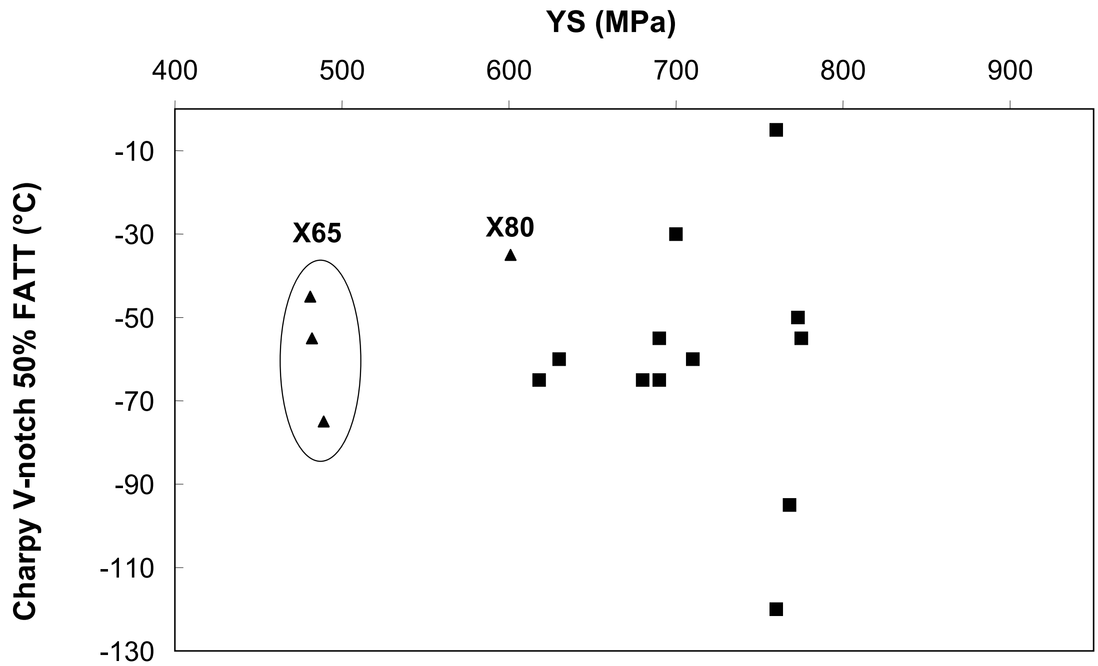


Figure 3. Strength-toughness combination of selected materials.

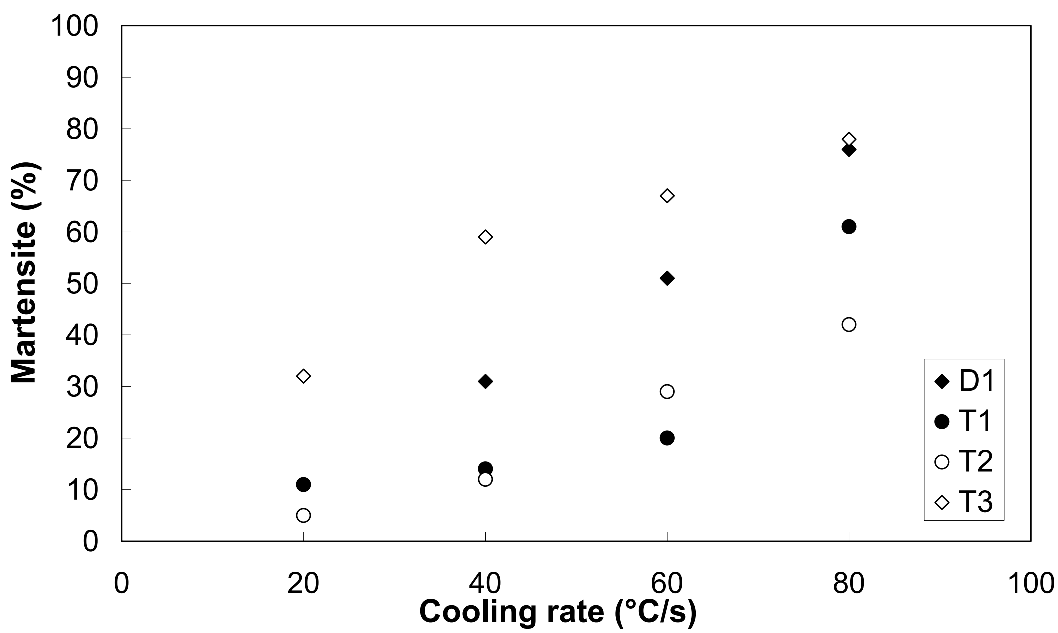


Figure 4. Martensite content as a function of cooling rate for steels with various Cr and Mo contents.

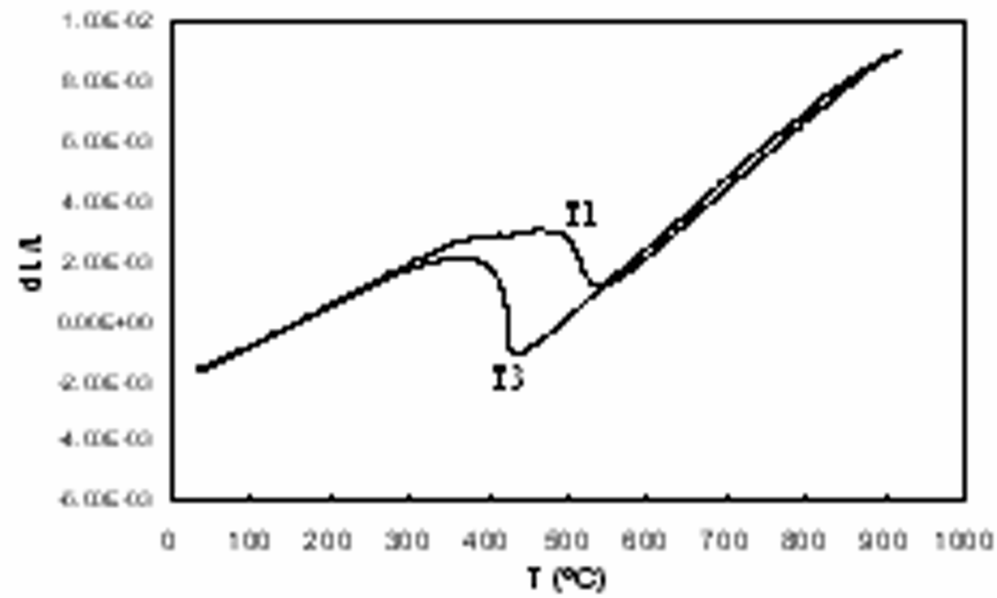


Figure 5. Dilatometric curves of steels T1 and T3. CR= 80 °C/s.

Microstructure of as-quenched materials

15-16 mm thickness. Similar average prior austenite grain size of 13 to 15 µm were found in all the considered materials. However, due to differences in chemical composition and some changes in cooling rates during heat treatment, different microstructures were formed.
For instance, a predominantly low carbon martensite microstructure was formed in the case of steels D1 and S2, whilst bainite was developed in steel T1, likely due to a slightly lower cooling rate during heat treatment, and steel S1 with the lowest hardenability.
Improved steel hardenability is associated with higher volume fractions of low carbon martensite, (e.g. steel T2 vs steel T1), whereas minor changes were seen when quenching at very high cooling rates of 15 mm thick material (e.g. steel D2 vs steel D1). A microstructure of 100 percent low carbon martensite was obtained in steel T3, which exhibits the highest hardenability.

Examples of microstructures developed in steel T1 (prevalently bainitic) and steel T3 (fully martensitic), as obtained by means of SEM, are shown in Figure 6.

| 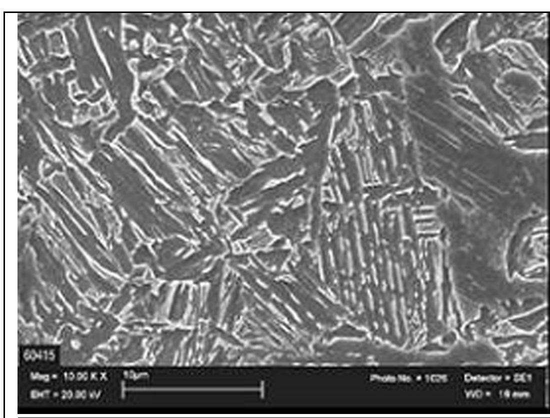 | 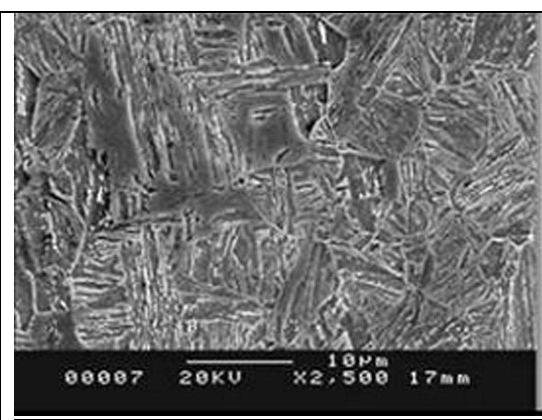 |
| --- | --- |
| Steel T1 | Steel T3 |

Figure 6. SEM image of as-quenched microstructures of steels T1 and T3, 16 mm thickness.

25 mm thickness. Slightly coarse AGS (18-21 µm) was measured in comparison with the 15-16 mm thick materials.

The following microstructures were observed:

(i) Predominantly coarse granular bainite (GB) for steels T1 and S2.

(ii) Improved steel hardenability helps to replace granular bainite with lower bainite in the case of steel T2 with respect to T1; low-C martensite was developed in steel D2, but islands of high carbon martensite and retained austenite (MA constituent) were still present.

(iii) 70 percent low carbon martensite and 30 percent bainite microstructure was obtained in steel T3.

Precipitation in Quenched and Tempered (Q&T) steels

Q&T materials exhibited a large number of precipitates. Particles located at grain boundaries were mainly $M_3C$ type (90%Fe-8%Mn-2%Cr), ranging in size from 50 to 300 nm, whilst within laths and grains also small precipitates (size from 10 to 40 nm), rich in niobium and molybdenum were revealed. Also vanadium was detected in these small precipitates. A different precipitation evolution was observed during tempering, depending on the as-quenched microstructures: precipitation of $M_3C$ was detected at grain and lath boundaries and at high-angle boundaries in lath martensite and bainite, respectively. In any case $M_3C$ precipitates seem too small to be initiation sites for cleavage fracture.

The average size of fine precipitates was measured by TEM to evaluate precipitation strengthening according to the Orowan relationship [5]. Values of 80 to 120 MPa were estimated. The greater strengthening (20-30 MPa) exhibited by steels D1 and D2, compared with steels T1, T2, and T3, derives from a higher frequency of finer precipitates. However, such contribution is not able to explain the differences in terms of strength between the considered materials.

Microstructure of Q&T steels

OIM examinations showed that Q&T materials, deriving from different as-quenched microstructures, are characterized by different misorientation distributions Figure 7:

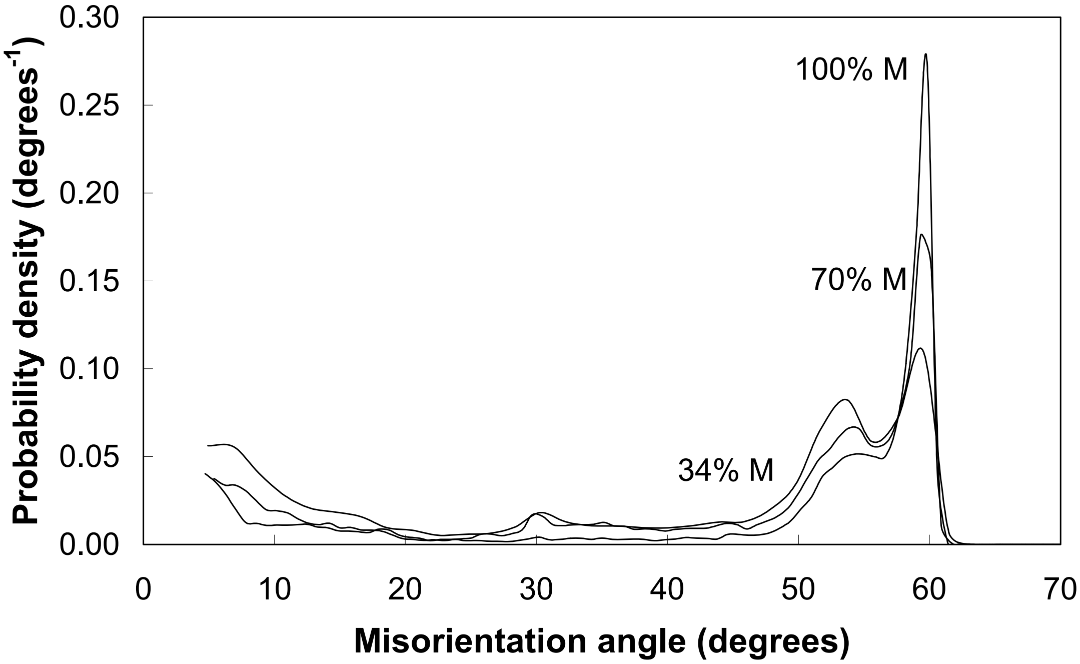


Figure 7. Misorientation profiles of materials with different martensite contents after quenching.

- In all cases very few boundaries were found with misorientation angle in the range 10°-50°.
- Predominantly bainitic microstructures, exhibit preferential misorientations in the range 47°-60°. Such orientations are compatible with Nishiyama-Wassermann misorientation relationships for packets coming from different $\{111\}_\gamma$ planes [6].
- Martensitic microstructures show a stronger peak at 60°. It is reported in the literature [7, 8] that this aspect is typical of misorientation related twins associated with self-accomodating martensite variants.

Considering the relationship between transgranular fracture and the presence of boundaries with a misorientation angle greater than 50° proposed by Watanabe [9], on the basis of the current results, bainitic or martensitic covariant packets and cells (*i.e.* regions separated by low-angle boundaries or subgrains) were defined as those regions misoriented more than 50 degrees and more then 2 degrees from their neighbours, respectively.

Examples of inverse pole figure maps of microstructures with increasing amounts of martensite are reported in Figure 8.

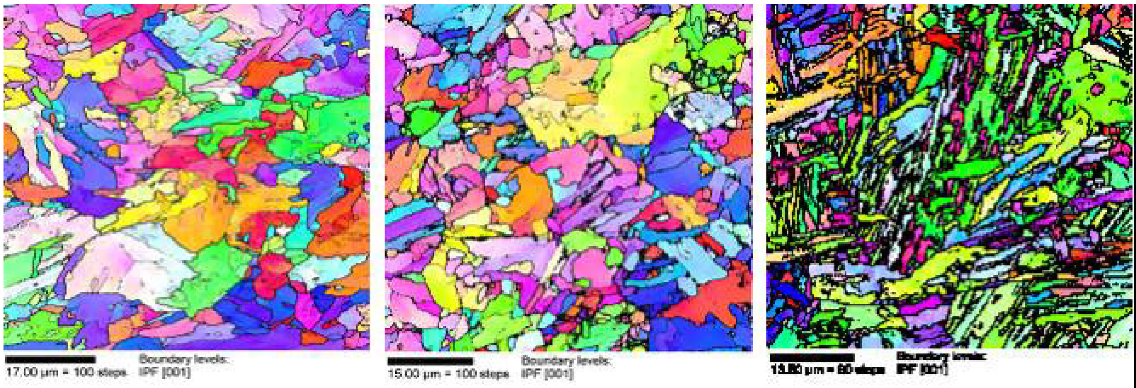


Bainitic microstructure (M < 20%) | Mixed bainitic-martensitic microstructure | Fully martensitic microstructure

Figure 8. Inverse pole figure map of Q&T materials with predominantly bainite, mixed martensite and bainite, and martensite microstructures, respectively, after quenching.

From such maps both packet and subgrain average sizes were measured.
The trend of packet size versus AGS is shown in Figure 9. Results indicate that:

- In predominantly bainitic microstructures (M < 20%), the packet size tends to increase with AGS coarsening
- In martensitic microstructures (M > 60%), the packet size slightly decreases as AGS increases.

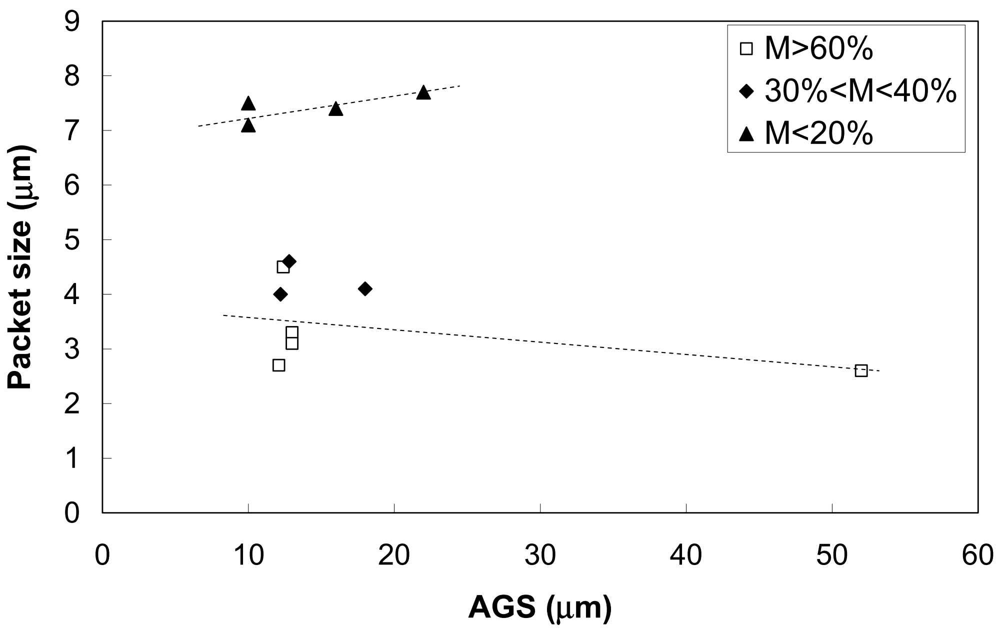


Figure 9. Bainite packet size versus austenite grain size (AGS).

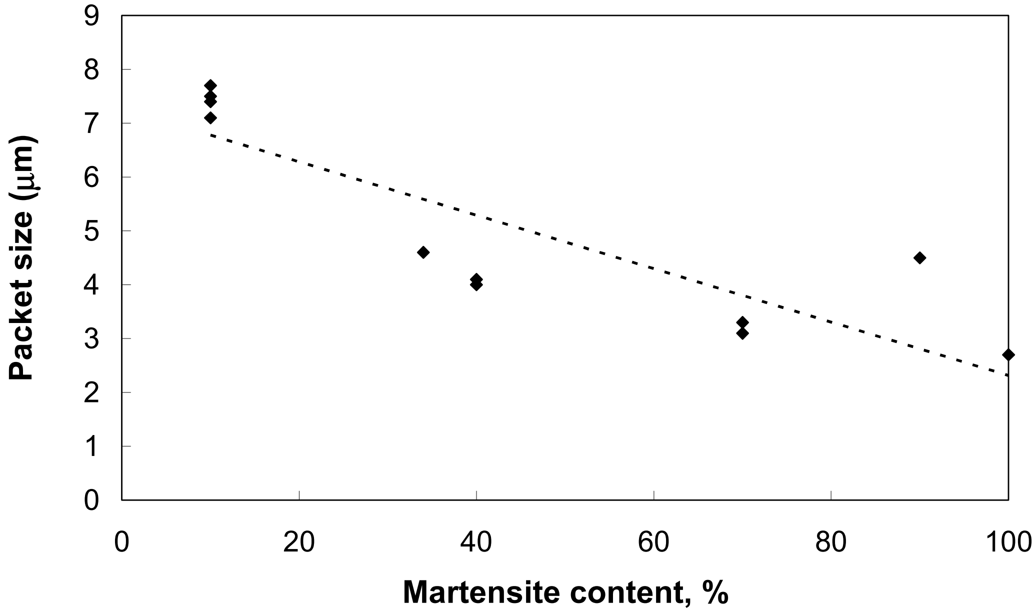


Figure 10. Packet size versus martensite content after quenching.

The data presented in Figure 10 show that the average packet size in the Q&T microstructure decreases as the martensite content in the as-quenched material increases.

Effect of Microstructure on Strength and Toughness

In order to compare the toughness of materials with different strength levels, a normalized value of 50% FATT, referred to a same yield strength value, was estimated using the relationship [10]:

$$\frac{\Delta FATT}{\Delta YS} = 0.3 \ \text{°C/MPa} \tag{1}$$

Resulting toughness correlated with the inverse square root of the packet size (Figure 11).

According to the classical model for cleavage fracture, which dictates that the critical stage for cleavage cracking is the propagation of a small crack originated in a single packet to the adjacent one, high-angle boundaries delimitating packets are effective barriers to crack propagation. Moreover, the finer the packet the smaller the incipient crack, that is the smaller the possibility for such crack to reach the “critical” size for propagation.

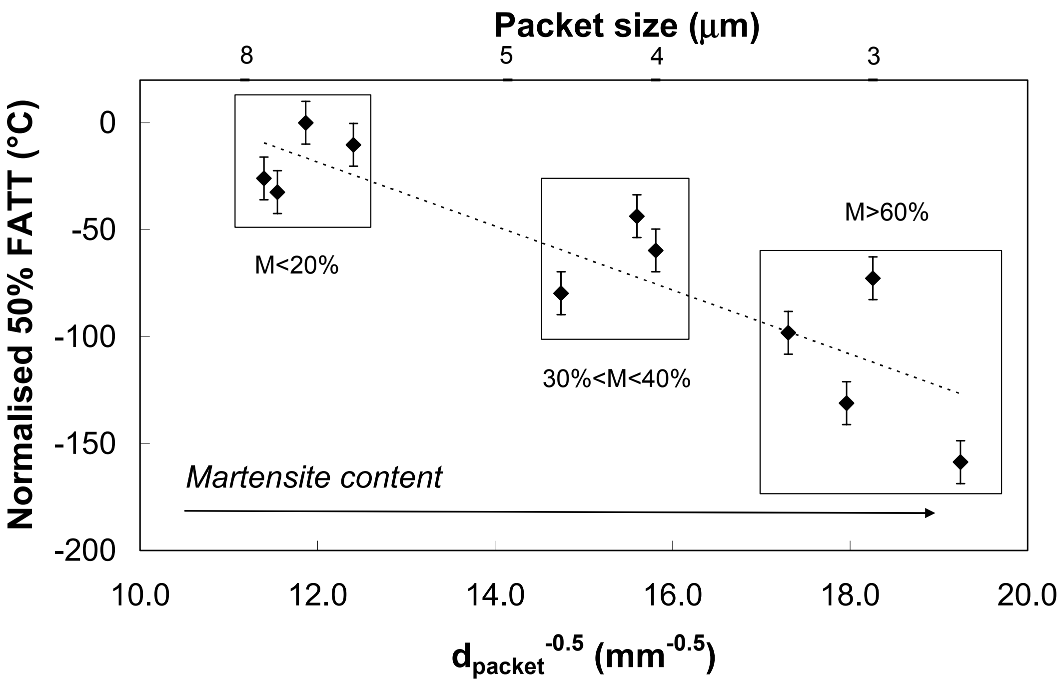


Figure 11. Toughness versus packet size for the considered Q&T materials.

On the other hand, sub-grain (low-angle) boundaries delineating cells are effective barriers to dislocation movement, thus determining the yield strength.

Based on the above proposed mechanism, the yield strengths of the materials were plotted against the inverse square root of the subgrain size ($d$), according to the Hall-Petch relationship [11]:

$$YS = YS_0 + k_y\, d^{-1/2} \tag{2}$$

Results, reported in Figure 12, show that:

- Yield strength follows Equation (2) with $k_y$ = 21.5 MPa mm$^{-1/2}$. This coefficient appears to be independent of microstructure and similar to that found for ultra-fine grained steel [12].
- The cell size decreases as the martensite content in the as-quenched material increases, with consequent strengthening.

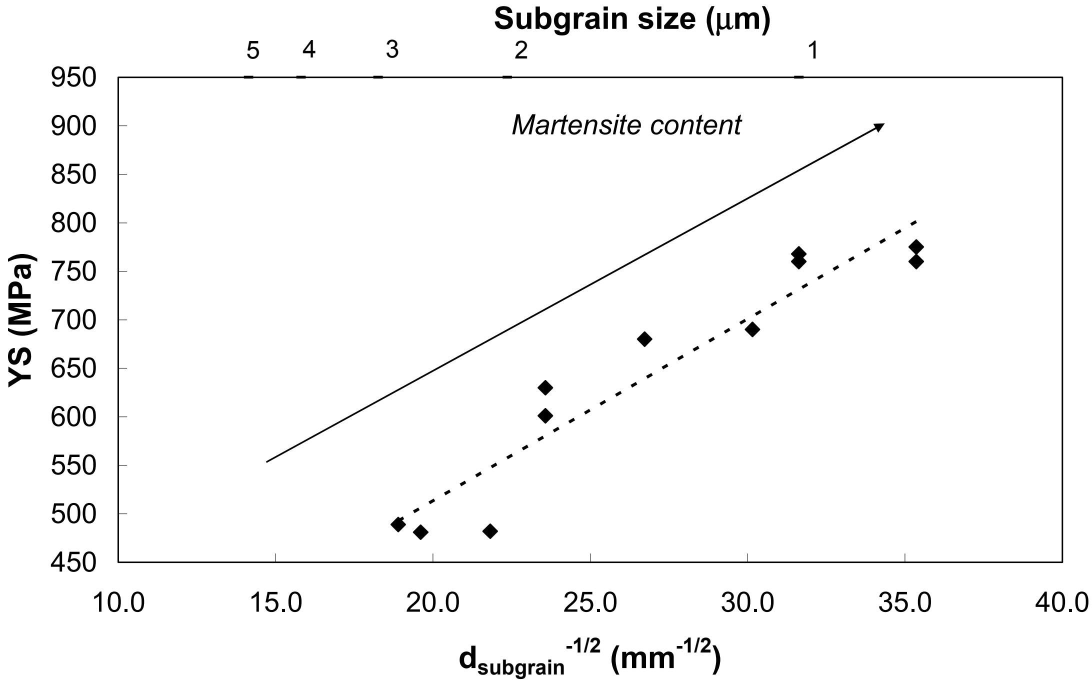


Figure 12. Dependence of yield strength on subgrain size for the considered Q&T materials

## Conclusions

The main microstructural features controlling the strength-toughness combination in these high strength Q&T steels have been established by advanced metallographic techniques:

- Sub-grain size is the key microstructural parameter defining the yield strength of the various materials.
- Toughness is related to the inverse square root of the packet size.
- For a given prior austenite grain size, the increase of the martensite volume fraction formed after quenching leads to a finer packet, thereby enhancing toughness.
- Fine packets and sub-grains, suitable for obtaining the target strength-toughness combination, i.e YS > 690 MPa (100 ksi) and FATT < – 50 °C (– 45 °F), were obtained when the as-quenched microstructure was mainly constituted of low-C martensite (M > 60%).

These results can be used to establish a production route for Q&T seamless pipes for deepwater TTR of 90 to 100 ksi grade. In particular, a steel containing 0.10% C, 1.50% Mn, 0.025% Nb and proper combinations of Mo, Cr and Ni (Ceq < 0.50%) is sufficient to develop Grade 100 ksi strengths in the case of 15 mm thick pipes and 90 ksi grade in 25 mm wall thickness pipes. A more robust chemical composition is needed to achieve 100 ksi yield strength in 25 mm thick pipes.

## References


1. E. Anelli, D. Colleluori, M. Pontremoli, G. Cumino, A. Izquierdo, H. Quintanilla (Paper presented at the Proc. 4th Int. Conf. on Pipeline Technology, Ostend, Belgium, 2004), 1679.
2. M. Tivelli, G. Cumino, A. Izquierdo, E. Anelli and A. Di Schino, "Metallurgical Aspects of Heavy Wall - High Strength Seamless Pipes for Deep Water Applications" (Paper presented at Rio Pipeline Conference & Exposition 2005, Rio de Janeiro, Brasil, 17-19 October 2005).
3. A. Di Schino, E. Anelli G. Cumino, M. Tivelli and A. Izquierdo, "Development of high strength quenched and tempered seamless pipes" (Paper presented at 1st Super High Strength Steel Conference, Rome, Italy, 2-4 November 2005).
4. E. Anelli, M.C. Cesile and P.E. Di Nunzio, "Prediction of austenite decomposition during cooling of low and medium-carbon low-alloy steels" (Paper presented at Modeling Control and optimization in Ferrous and non Ferrous industry Conference, Chicago, USA, 9-12 November 2003).
5. P. Haasen, *Physical Metallurgy* (Cambridge University Press, 1996), 258.
6. A.F. Gourges, H.M. Flower and T.C. Lindley, *Materials Science and Technology*, 16, (2000), 26.
7. P.M. Kelly, *Acta Metallurgica*, 13, (1965), 365.
8. P.M. Kelly, *Materials Transaction*, 33, (1992), 235.
9. T. Watanabe and S. Tsurekawa, *Acta Materialia,* 15, (1999), 4171.
10. P. Brozzo, G. Buzzichelli, A. Mascanzoni and M. Mirabile, *Metal Science*, 11, (1977), 123.
11. N.J. Petch, *J. Iron & Steel Inst.*, 174, (1953), 25.
12. S. Takaki, S. Nakamura, *COMP-ISIJ*, 12, (1999), 361.